

Quantum dynamics of an electromagnetic mode that cannot contain N photons

L. Bretheau,¹ P. Campagne-Ibarcq,¹ E. Flurin,¹ F. Mallet,¹ and B. Huard^{1,*}

¹*Laboratoire Pierre Aigrain, Ecole Normale Supérieure-PSL Research University, CNRS, Université Pierre et Marie Curie-Sorbonne Universités, Université Paris Diderot-Sorbonne Paris Cité, 24 rue Lhomond, 75231 Paris Cedex 05, France*

Electromagnetic modes are instrumental in building quantum machines. In this experiment, we introduce a method to manipulate these modes by effectively controlling their phase space. Preventing access to a single energy level, corresponding to a number of photons N , confined the dynamics of the field to levels 0 to $N - 1$. Under a resonant drive, the level occupation was found to oscillate in time, similarly to an N -level system. Performing a direct Wigner tomography of the field revealed its nonclassical features, including a Schrödinger cat-like state at half period in the evolution. This fine control of the field in its phase space may enable applications in quantum information and metrology.

The manipulation of a quantum system usually involves the control of its Hamiltonian in time. An alternative route consists in effectively tailoring its Hilbert space dynamically. This can be done by restricting the system evolution to a subset of possible states. When even a single energy level is disabled, the system evolution is deeply modified and is ruled by the so-called quantum Zeno dynamics (QZD) [1–5]. As the name suggests, the level blockade can be realized by repeatedly checking whether the level is occupied, owing to the inherent back action of quantum measurements [1, 2, 6]. Alternatively, as in the present experiment, QZD can be achieved by blocking the level using a strong, active coupling to an ancillary quantum system [3–5], without any measurement [7]. These ideas have recently been demonstrated for atoms, using either Rb Bose-Einstein condensates [8] or Rydberg atoms [9]. However, the dynamics of these systems is intrinsically confined to a finite number of energy levels. Here, using a circuit quantum electrodynamics architecture, we implement QZD of light. With its large number of energy levels and ease of control, a single electromagnetic mode offers a wider and more controllable phase space than atoms and two-level systems.

The principle of our experiment is shown in Fig. 1. One cavity mode of frequency f_c is coupled to a qubit of frequency f_q . For large enough detuning, their evolution can be described by the dispersive Hamiltonian $hf_c a^\dagger a + hf_q |e\rangle\langle e| - h\chi a^\dagger a |e\rangle\langle e|$, where h is Planck's constant, a^\dagger is the ladder operator and $|e\rangle$ is the excited state of the qubit. The last term describes the frequency shift of the cavity (qubit) by $-\chi$, which occurs when the qubit (cavity) is excited by one extra quantum of energy. Owing to this shift, a tone at frequency $f_q - N\chi$ addresses only the transition between states $|N\rangle \otimes |g\rangle$ and $|N\rangle \otimes |e\rangle$ for level widths smaller than χ [10]; here $|g\rangle$ is the ground state of the qubit. These levels then hybridize and repel each other. Their splitting is given by the Rabi frequency Ω_R at which the qubit population would oscillate in the case where the cavity is in state $|N\rangle$ (Fig. 1). Any transi-

tion to level N is now forbidden when the cavity is driven at resonance. Schematically, level N has been moved out of the harmonic ladder (Fig. 1). Then, starting from the ground state, the electromagnetic mode is confined to levels 0 to $N - 1$, whereas the qubit remains in its ground state. The field dynamics is dramatically changed, resembling that of an N -level system, and nonclassical states similar to Schrödinger cat states develop.

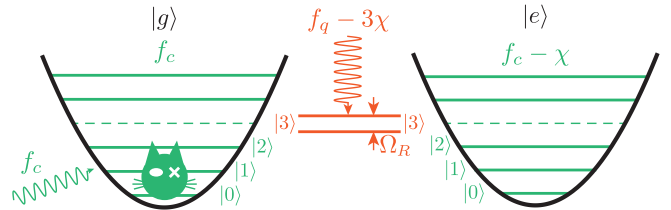


Figure 1: Principle of the experiment. Combined energy level diagram of the cavity coupled to the ancillary qubit. Each state is labelled as $|k\rangle \otimes |g/e\rangle$ for k photons in the cavity and the qubit either in the ground (g) or excited (e) states. The level $N = 3$ is dynamically blocked by driving the qubit transition at $f_q - N\chi$ (red wave). This drive hybridizes the states $|N\rangle \otimes |g\rangle$ and $|N\rangle \otimes |e\rangle$ and shifts their energy. A coherent excitation at the cavity frequency f_c (green wave) induces a periodic evolution of the field confined to the first N levels. At half period, a nonclassical state similar to a Schrödinger cat is produced.

In the experiment, we use the fundamental mode of a three-dimensional (3D) microwave cavity made out of bulk aluminum, which resonates at $f_c = 7.804$ GHz. This mode is off-resonantly coupled to a superconducting qubit [11] with bare frequency $f_q = 5.622$ GHz and dispersive frequency shift $\chi = 4.63$ MHz. The cavity exit rate $\gamma_c = (1.3 \mu\text{s})^{-1}$ is dominated by the coupling rate to two transmission lines connected to the cavity, which are used for both driving and the readout of the system. The relaxation rate $\gamma_1 = (11.5 \mu\text{s})^{-1}$ and decoherence rate $\gamma_2 = (8.9 \mu\text{s})^{-1}$ of the ancillary qubit are an order of magnitude smaller.

The experiment is performed by first turning on the blocking tone at $f_q - N\chi$. For the level blockade to be effective, we choose $\Omega_R = 6.24$ MHz much larger than

*Corresponding author. E-mail: benjamin.huard@ens.fr

the level frequency width, which is about γ_c . Then the cavity is driven at frequency $f_d \approx f_c$ for a time t varying up to a few μs . The drive power is fixed throughout the experiment and would lead to an amplitude displacement rate ϵ_d of about $3 \mu\text{s}^{-1}$ in the cavity, were there neither damping nor nonlinearities. At time t , both the blocking signal and the cavity drive are turned off, and the field state is measured. Two measurement schemes are used to characterize the cavity state. Both methods use as a probe the same qubit that is used to provide the level blockade.

The first method consists in measuring the probability P_k for the field to host k photons. To do so, a selective π pulse is applied to the qubit at frequency $f_q - k\chi$ so that it gets excited if k photons are in the cavity. Measuring the probability to find the qubit in the excited state hence gives P_k [12]. This direct measurement relies on the qubit being initially in the ground state, which is not always the case. To account for this, two spurious effects need to be considered. First, the qubit has a residual thermal population of 22 %. Second, imperfections of the blockade induce a parasitic excitation of the qubit, which was measured in time and remains below 18 %. Taking these effects into account leads to an accurate determination of the conditional probability \tilde{P}_k of measuring k photons, given the qubit being initially in the ground state citeFootnote2.

The resulting probabilities are shown in Fig. 2 as a function of time for several photon numbers k and for N from 2 to 5. Levels with more than N photons are unoccupied, as expected from Hilbert space blockade. Early in the evolution, the occupation of the levels $k \geq 1$ rises in the order of increasing energy, similarly to a coherent state of increasing amplitude (Fig. S3c in [13]). Later, the level distribution "bounces" off a wall at $k = N$, so that the probabilities start to oscillate. The period of the oscillations increases with N as expected, because it takes more time to reach $N - 1$ photons with a constant drive as N increases. The case $N = 2$ is straightforward as it implements an effective qubit [8]. The time traces of Fig. 2 correspond to Rabi oscillations of a two-level system. For larger N , the evolution is similar to that of a resonantly driven N -level system, as seen in Rydberg atoms [9]. In particular, at half period, \tilde{P}_0 displays plateaus all the more pronounced as N gets larger. Finally, the $N - 1$ level occupation evolves in opposition to level 0, with a maximum at half period.

The evolution of the field can be modeled with the Hamiltonian of the cavity

$$H = i\hbar\epsilon_d(a_N^\dagger - a_N)/2\pi + \hbar(f_c - f_d)a_N^\dagger a_N - \hbar\lambda(a_N^\dagger)^2 a_N^2, \quad (1)$$

written in the frame rotating at the drive frequency f_d . These three terms describe the coherent drive, its detuning, and the nonlinearity of the cavity, respectively. The blockade at level N suppresses transitions to and from $|N\rangle$. This is entirely modeled by an effective annihila-

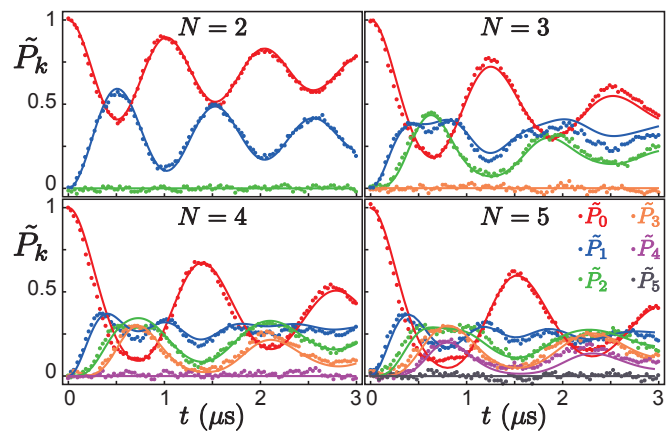


Figure 2: **Evolution of the photon number probabilities.** Measured (dots) and theoretical (solid lines) photon number state probabilities \tilde{P}_k as a function of time t . The blocked level N ranges from 2 to 5 and is indicated on each panel. The standard deviation, estimated from the curve $\tilde{P}_N(t)$, is below 1.7%.

tion operator

$$a_N = a - \sqrt{N}|N-1\rangle\langle N| - \sqrt{N+1}|N\rangle\langle N+1|, \quad (2)$$

for which these forbidden transitions are removed. Finally, the relaxation at rate γ_c is modeled using a master equation of Lindblad form [13].

Using this model, one can reproduce with good agreement the photon number probabilities \tilde{P}_k (Fig. 2), with the displacement rate ϵ_d , the drive detuning $f_c - f_d$, and the cavity anharmonicity λ as the fit parameters. The displacement rate ϵ_d , which directly determines the period of oscillations in the level occupation (Fig. 2), is found to be finely tuned between 2.83 and $3.05 \mu\text{s}^{-1}$ for each blocked level N . The anharmonicity $\lambda = -70$ kHz is negative, as confirmed by independent measurements (Fig. S2 in [13]). This negativity is in contradiction to all reported transmon qubit and 3D transmon models such as those in Refs. [14–16]. At last, we attribute the origin of the detuning $f_c - f_d$ to an energy shift of the levels caused by the blocking tone. It was found to be -0.1 MHz for $N > 2$ and -0.4 MHz for $N = 2$. These values are consistent with the system being more strongly disturbed by the blocking field at $N = 2$ than for larger N .

These measurements demonstrate how the cavity is transformed into an N -level system by dynamically inducing a blockade at an arbitrary level N . A full characterization of the field, which goes beyond measuring only photon number probability, requires tomography. The Wigner function is a complete representation of the quantum state of the field in continuous variables. It can be expressed as $W(\alpha) = \langle D_\alpha \mathcal{P} D_\alpha^\dagger \rangle$, where $D_\alpha = e^{\alpha a^\dagger - \alpha^* a}$ is the field displacement operator and $\mathcal{P} = e^{i\pi a^\dagger a}$ the photon parity operator. A direct Wigner tomography of the field is thus performed by first displacing it by a complex

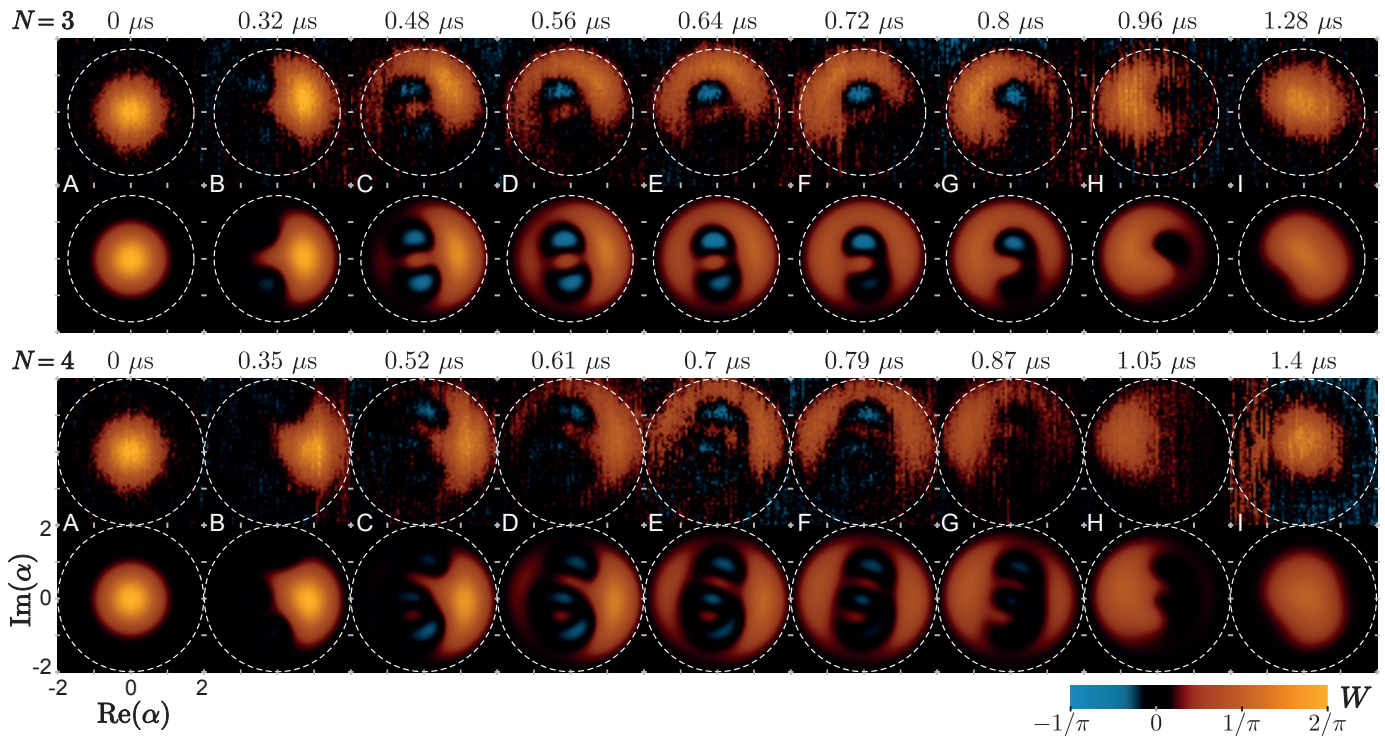


Figure 3: **Time evolution of the Wigner function of a quantum mode of light under QZD.** Measured (top rows) and predicted (bottom rows) Wigner functions $W(\alpha)$ as a function of the displacement amplitude α , for a blockade at $N = 3$ (top panel) and $N = 4$ (bottom panel). The time t (nonlinear scale) for the frames shown in **A** to **I** is given above each panel. The field is confined in phase space by a barrier at amplitude $|\alpha| = \sqrt{N}$ (white dashed circle). Negative values of the Wigner function, in blue, demonstrate the nonclassical nature of the field produced under QZD. The model used is the same as for Fig. 2. Wigner functions are directly measured here and not reconstructed.

amplitude α and then measuring the average photon parity. This can be realized by mapping even and odd photon numbers on the qubit ground and excited states [17–19]. In practice, this is performed in three steps. The qubit is first prepared in state $(|g\rangle + |e\rangle)/\sqrt{2}$ using a pulse at the qubit frequency. The $\pi/2$ pulse bandwidth is designed to be larger than 10χ so as to succeed regardless of the cavity state. Then, the qubit is left to evolve freely during a time τ , where it acquires a phase shift that depends on the cavity state owing to the evolution operator $e^{i2\pi\chi\tau a^\dagger a|e\rangle\langle e|}$. The waiting time is chosen to be $\tau = 1/2\chi = 108$ ns, so that the qubit phase increases by $k\pi$ when the cavity state is $|k\rangle$ (Fig. S4 in [13]). Finally, another broadband $\pi/2$ pulse is applied in order to flip the qubit to the excited (ground) state in case of an even (odd) number of photons. Measuring the qubit state then directly leads to the Wigner function in contrast to indirect reconstruction procedures such as maximum likelihood.

The measured Wigner functions for the field state are shown in Fig. 3 at various times during the first oscillation period for blocked levels $N = 3$ and $N = 4$. At time zero (Fig. 3A), the cavity is in the vacuum state and the Wigner function is a positive Gaussian distribution centered at $\alpha = 0$, with a width reflecting zero

point fluctuations. As time increases, the resonant drive displaces the Wigner function along the real and positive axis. Without the blockade, and neglecting losses and anharmonicity, the vacuum state observed at time 0 would simply get displaced by $\alpha = \epsilon_d t$. In the presence of the blockade at level N , all levels with $k \geq N$ remain empty so that the field cannot be in a coherent state, and the distribution gets distorted. Indeed in Fig. 3B, the quasi-probability distribution seems to hit a wall in phase space at an amplitude \sqrt{N} . There, it undergoes a rapid counterclockwise evolution (Fig. 3C to H) along the corresponding barrier (white dashed circle). After a full oscillation period (Fig. 3I), the cavity goes back to a state close to the vacuum state of Fig. 3A. These snapshots of the field state are close to the ones predicted in Ref [5] for light under QZD, and similar to the one observed in the levels of a Rydberg atom [9].

Besides confirming the confined and periodic evolution of the field under QZD, this tomography reveals the formation of nonclassical field states, as indicated by the appearance of negative values in the Wigner function. These negative values develop while the field undergoes a transition along the barrier in phase space. At half period, the state is close to an equal superposition of positive and negative field amplitudes at $\pm\sqrt{N-1}$. The quantum nature of this superposition manifests itself by

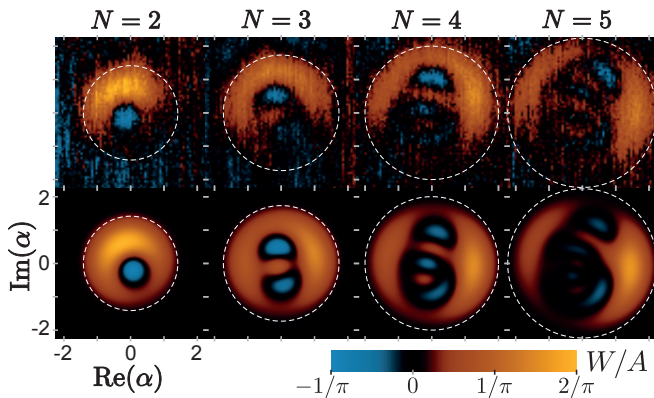


Figure 4: **Wigner tomography at half period.** Measured (top row) and calculated (bottom row) Wigner functions of the cavity field for various blockade levels N from 2 to 5, taken at half period ($t = 0.51 \mu\text{s}, 0.64 \mu\text{s}, 0.7 \mu\text{s}$ and $0.75 \mu\text{s}$). The color scale is rescaled compared with Fig. 3 by $A = 0.7$. Similarly to Schrödinger cat states, these states exhibit fringes with alternating positive and negative values.

the appearance of interference fringes in the Wigner function. These characteristic patterns can be compared for all blockade levels $2 \leq N \leq 5$ in Fig. 4. The photon parity is that of the highest allowed level $N - 1$, which is also the number of negative fringes. These properties are reminiscent of a quantum superposition between two coherent states of amplitude $\pm\sqrt{N-1}$, so-called Schrödinger cat state [20]. The evolution of the Wigner function can be predicted using the model above. The calculated dis-

tributions are shown below each measurement frame in Figs. 3 and 4. The observed asymmetry between positive and negative imaginary amplitudes is attributed to drive detuning, losses and anharmonicity [12, 20]. The model reproduces qualitatively the measured Wigner functions for all times and values of N .

In conclusion, we have demonstrated Quantum Zeno Dynamics of microwave light. Our experiment shows that a mode that cannot contain N photons undergoes a coherent evolution that is confined in phase space. Effectively, an electromagnetic mode is transformed into an $N/2$ spin. As a result of this transformation, exotic non-classical states develop under a simple resonant drive and share similar features with Schrödinger cat states of light. Our work could be extended to allow evolution outside of the exclusion circle, where the barrier acts as a peculiar scatterer in phase space [5]. Other cat-like states and squeezed states could then be produced. Tailoring the Hilbert space in time is an important new resource for quantum control. Our experiment enables the realization of various protocols based on QZD, such as generation and protection of entanglement [21–23], and quantum logic operations [24]. Moreover, by turning on and off in time the blockade level and combining it with fast amplitude displacements, which is feasible by improving the cavity decay rate by an order of magnitude, it would be possible to realize phase space tweezers for light [4, 5]. A possible and important outcome would then be the manipulation of Schrödinger cat states in a unique way and the quantum error correction of cat-qubits, which are a promising quantum computing paradigm [25].

-
- [1] P. Facchi, V. Gorini, G. Marmo, S. Pascazio and E. C. G. Sudarshan. Quantum Zeno dynamics. *Phys. Lett. A* **12**–**19** (2000).
 - [2] P. Facchi and S. Pascazio. Quantum Zeno Subspaces. *Phys. Rev. Lett.* **89**, 080401 (2002).
 - [3] P. Facchi, D. Lidar and S. Pascazio. Unification of dynamical decoupling and the quantum Zeno effect. *Phys. Rev. A* **69**, 032314 (2004).
 - [4] J. M. Raimond, C. Sayrin, S. Gleyzes, I. Dotsenko, M. Brune, S. Haroche, P. Facchi and S. Pascazio. Phase Space Tweezers for Tailoring Cavity Fields by Quantum Zeno Dynamics. *Phys. Rev. Lett.* **105**, 213601 (2010).
 - [5] J. M. Raimond, P. Facchi, B. Peaudecerf, S. Pascazio, C. Sayrin, I. Dotsenko, S. Gleyzes, M. Brune and S. Haroche. Quantum Zeno dynamics of a field in a cavity. *Phys. Rev. A* **86**, 032120 (2012).
 - [6] B. Misra and E. C. G. Sudarshan. The Zeno’s paradox in quantum theory. *J. Math. Phys.* **18**, 756 (1977).
 - [7] Originally, QZD corresponded to quantum evolutions restricted by measurement. Yet, the name was later extended to any quantum dynamics in a restricted Hilbert space [3].
 - [8] F. Schäfer, I. Herrera, S. Cherukattil, C. Lovecchio, F. S. Cataliotti, F. Caruso and A. Smerzi. Experimental realization of quantum zeno dynamics. *Nat. Commun.* **5**, 3194 (2014).
 - [9] A. Signoles, A. Facon, D. Grosso, I. Dotsenko, S. Haroche, J.-M. Raimond, M. Brune and S. Gleyzes. Confined quantum Zeno dynamics of a watched atomic arrow. *Nat. Phys.* **10**, 715–719 (2014).
 - [10] D. I. Schuster, A. A. Houck, J. A. Schreier, A. Wallraff, J. M. Gambetta, A. Blais, L. Frunzio, J. Majer, B. Johnson, M. H. Devoret, S. M. Girvin and R. J. Schoelkopf. Resolving photon number states in a superconducting circuit. *Nature* **445**, 515–8 (2007).
 - [11] H. Paik, D. I. Schuster, L. S. Bishop, G. Kirchmair, G. Catelani, A. P. Sears, B. R. Johnson, M. J. Reagor, L. Frunzio, L. I. Glazman, S. M. Girvin, M. H. Devoret and R. J. Schoelkopf. Observation of High Coherence in Josephson Junction Qubits Measured in a Three-Dimensional Circuit QED Architecture. *Phys. Rev. Lett.* **107**, 240501 (2011).
 - [12] G. Kirchmair, B. Vlastakis, Z. Leghtas, S. E. Nigg, H. Paik, E. Ginossar, M. Mirrahimi, L. Frunzio, S. M. Girvin and R. J. Schoelkopf. Observation of quantum state collapse and revival due to the single-photon Kerr effect. *Nature* **495**, 205–9 (2013).
 - [13] Materials and methods are available as supplementary material on Science Online.
 - [14] S. E. Nigg, H. Paik, B. Vlastakis, G. Kirchmair, S. Shankar, L. Frunzio, M. H. Devoret, R. J. Schoelkopf and S. M. Girvin. Black-Box Superconducting Circuit

- Quantization. *Phys. Rev. Lett.* **108**, 240502 (2012).
- [15] J. Bourassa, F. Beaudoin, J. M. Gambetta and a. Blais. Josephson-junction-embedded transmission-line resonators: From Kerr medium to in-line transmon. *Phys. Rev. A* **86**, 013814 (2012).
- [16] F. Solgun, D. W. Abraham and D. P. DiVincenzo. Black-box quantization of superconducting circuits using exact impedance synthesis. *Phys. Rev. B* **90**, 134504 (2014).
- [17] L. Lutterbach and L. Davidovich. Method for Direct Measurement of the Wigner Function in Cavity QED and Ion Traps. *Phys. Rev. Lett.* **78**, 2547–2550 (1997).
- [18] P. Bertet, a. Auffeves, P. Maioli, S. Osnaghi, T. Meunier, M. Brune, J. Raimond and S. Haroche. Direct Measurement of the Wigner Function of a One-Photon Fock State in a Cavity. *Phys. Rev. Lett.* **89**, 200402 (2002).
- [19] B. Vlastakis, G. Kirchmair, Z. Leghtas, S. E. Nigg, L. Frunzio, S. M. Girvin, M. Mirrahimi, M. H. Devoret and R. J. Schoelkopf. Deterministically encoding quantum information using 100-photon Schrödinger cat states. *Science* **342**, 607–10 (2013).
- [20] S. Haroche and J. M. Raimond. *Exploring the Quantum* (Oxford University Press, Oxford, 2006).
- [21] S. Maniscalco, F. Francica, R. L. Zaffino, N. Lo Gullo and F. Plastina. Protecting Entanglement via the Quantum Zeno Effect. *Phys. Rev. Lett.* **100**, 090503 (2008).
- [22] X.-B. Wang, J. Q. You and F. Nori. Quantum entanglement via two-qubit quantum Zeno dynamics. *Phys. Rev. A* **77**, 062339 (2008).
- [23] Z. C. Shi, Y. Xia, H. Z. Wu and J. Song. One-step preparation of three-particle Greenberger-Horne-Zeilinger state via quantum Zeno dynamics. *Eur. Phys. J. D* **66**, 127 (2012).
- [24] X.-Q. Shao, L. Chen, S. Zhang and K.-H. Yeon. Fast CNOT gate via quantum Zeno dynamics. *J. Phys. B At. Mol. Opt. Phys.* **42**, 165507 (2009).
- [25] M. Mirrahimi, Z. Leghtas, V. V. Albert, S. Touzard, R. J. Schoelkopf, L. Jiang and M. H. Devoret. Dynamically protected cat-qubits: a new paradigm for universal quantum computation. *New J. Phys.* **16**, 045014 (2014).

Acknowledgments We thank Michel Devoret, Sukhdeep Dhillon, Çağlar Girit, Takis Kontos, Zaki Leghtas, Vladimir Manucharyan, Mazyar Mirrahimi, Saverio Pascazio, the Quantronics Group, Jean-Michel Raimond, Pierre Rouchon, and Jérémie Viennot. Nanofabrication has been made within the consortium Salle Blanche Paris Centre. This work was supported by the ANR contract ANR-12-JCJC-TIQS and the Qumotel grant Emergences of Ville de Paris. LB acknowledges support from Direction Générale de l’Armement.

Supplementary Materials

www.sciencemag.org
 Materials and Methods
 Supplementary Text
 Figs. S1 to S4
 References [26-32]